Check for updates

Design, synthesis and bioactivity of myricetin derivatives for control of fungal disease and tobacco mosaic virus disease†

Xiao Cao, Bangcan He, Fang Liu, Yuanquan Zhang, Li Xing, Nian Zhang, Yuanxiang Zhou, Chenyu Gong and Wei Xue [ID] *

A series of myricetin derivatives containing isoxazole were designed and synthesized. All the synthesized compounds were characterized by NMR and HRMS. In terms of antifungal activity, **Y3** had a good inhibitory effect on *Sclerotinia sclerotiorum* (Ss), and the median effective concentration (EC_{50}) value was 13.24 μg mL^{-1}, which was better than azoxystrobin (23.04 μg mL^{-1}) and kresoxim-methyl (46.35 μg mL^{-1}). Release of cellular contents and cell membrane permeability experiments further revealed that **Y3** causes the destruction of the cell membrane of the hyphae, which in turn plays an inhibitory role. The anti-tobacco mosaic virus (TMV) activity *in vivo* showed that **Y18** had the best curative and protective activities, with EC_{50} values of 286.6 and 210.1 μg mL^{-1} respectively, the effect was better than ningnanmycin. Microscale thermophoresis (MST) data showed that **Y18** had a strong binding affinity with tobacco mosaic virus coat protein (TMV-CP), with a dissociation constant (K_d) value of 0.855 μM, which was better than ningnanmycin (2.244 μM). Further molecular docking revealed that **Y18** interacts with multiple key amino acid residues of TMV-CP, which may hinder the self-assembly of TMV particles. Overall, after the introduction of isoxazole on the structure of myricetin, its anti-Ss and anti-TMV activities have been significantly improved, which can be further studied.

1. Introduction

Plant pathogenic fungi and viral infections are highly infective and have a wide range of parasitic hosts, which seriously affect the quality and yield of crops and cause huge economic losses.[1–3] At present, the use of pesticides is still one of the most effective and economical means to control and treat plant diseases.[4,5] However, due to long-term use or unscientific abuse of these fungicides and antiviral agents, such as azoxystrobin, kresoxim-methyl, and ningnanmycin, plant diseases have developed drug resistance.[6,7] In addition, due to the high toxicity of these traditional pesticides, they are not easy to degrade, and they also cause certain damage to the ecological environment.[8,9] Therefore, it is of great interest to develop drug molecules with novel structures, environmental friendliness and highly effective bioactivity.

Myricetin is a natural dietary flavonoid that can be extracted from plants such as grapes and vine tea.[10] Relevant studies have shown that myricetin can regulate a variety of

physiological abnormalities, such as anticancer,[11] antiviral,[12–14] antioxidant,[15] analgesic[16] and anti-allergic.[17] In addition, our group found in previous studies that myricetin and its derivatives exhibit good biological activity in plant pathogenic bacteria and viruses,[9,18] which provides new ideas for the creation of new pesticides.

Isoxazole is a class of five-membered heterocyclic compounds containing nitrogen and oxygen atoms, which has attracted widespread attention with its excellent biological activity and unique structural characteristics.[19] Related studies have revealed that compounds containing isoxazole structures exhibit a wide range of biological functions. It not only has good anti-cancer[20] bactericidal,[21] antiviral[22,23] and anti-inflammatory,[24] biological activities in the field of medicine, but also shows excellent antifungal,[25] insecticidal,[26] herbicidal[27] and other biological activities in the field of pesticides.

In this study, the isoxazole was introduced into the structure of myricetin through the principle of active splicing, and a series of myricetin derivatives containing isoxazole were designed and synthesized. The design idea is shown in Fig. 1. Subsequently, the antifungal and anti-TMV activities of the synthesized target compounds were evaluated, and the mechanism of action of the compounds with excellent activity were preliminarily studied.

National Key Laboratory of Green Pesticide, Key Laboratory of Green Pesticide and Agricultural Bioengineering, Ministry of Education, Center for R&D of Fine Chemicals of Guizhou University, Guiyang 550025, P. R. China. E-mail: wxue@gzu. edu.cn; Fax: +86-851-88292090; Tel: +86-851-88292090
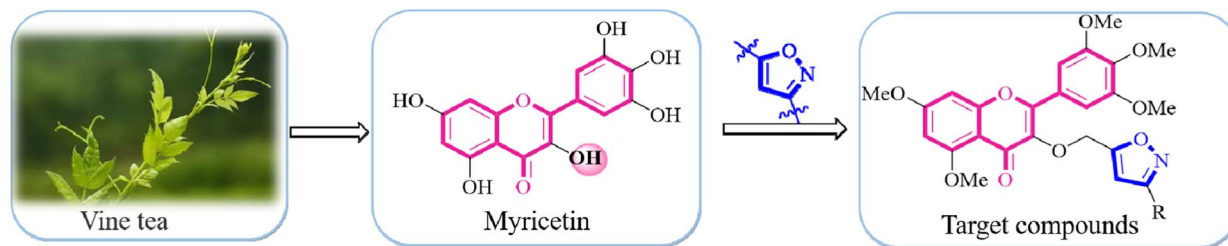
Fig. 1 The design ideas of target compounds.

2. Experimental

2.1 Instruments and chemicals

The melting point of the compounds were determined by X-4B melting point instrument (Shanghai INESA Co., Ltd.), without the correction. The target compounds **Y1–Y28** were characterized by nuclear magnetic resonance spectrometer with deuterated chloroform as solvent (Bruker, Germany) and Thermo Scientific Q Exactive Mass Spectrometer (Missouri, USA). The K_d values of compounds to TMV-CP were determined by using NanoTemper Monolith NT.115 microscale thermophoresis (NanoTemper, Germany). The chromatogram of **Y1** was determined by Agilent 1100 high performance liquid chromatography (HPLC) (Agilent, USA). The microstructure of **Y1** was observed by Olympus CX21 optical microscope (Olympus, Japan). All solvents and reagents were analytically or chemically pure, requiring no further purification, and the aldehyde containing compounds were purchased from the Shanghai Tansoole platform. Silica gel GF254 thin-layer chromatography was used to monitor the reaction progress.

2.1.1 Detection conditions of HPLC. The chromatography was performed on Lichrospher C_{18} column (250 mm × 4.5 mm, 5 μm) with mobile phase consisted of water–methanol (30 : 70 vol) at the flow rate of 1.00 mL min^{-1}. The detection wavelength was 280 nm and the sample size was 20 μL.

2.2 Synthesis

2.2.1 General procedures for preparing intermediates 1 to 4. The intermediates **1** to **4** were prepared according to the methods reported in the literature and slightly modified.[28–31] Firstly, various aldehydes were used as starting materials to react with $NH_2OH \cdot HCl$ to obtain intermediate **1**; secondly, it reacted with *N*-chlorosuccinimide (NCS) to obtain nitrile oxide intermediate **2**; then, the intermediate **3** was obtained by dipolar cycloaddition reaction with 3-bromopropyne; finally, methyl iodide was used as the methylation reagent to protect the hydroxyl group of myricitrin, and then deglycoside by concentrated hydrochloric acid to obtain intermediate **4**.

2.2.2 General procedures for preparing target compounds Y1–Y28. With *N*,*N*-dimethylformamide (DMF) as solvent and anhydrous K_2CO_3 as acid binding agent, intermediate **3** reacted with intermediate **4** at 60 °C for 4 h, and then recrystallizes the target compounds **Y1–Y28** by methanol. The specific synthesis process of the target compound **Y1–Y28** can be obtained from the ESI.†

2.3 Biological activities

2.3.1 Antifungal activity *in vitro*. The antifungal effect of the target compounds **Y1–Y28** *in vitro* was performed by the method reported in the literature.[32] Commercial fungicides kresoxim-methyl and azoxystrobin were used as positive controls, and the experiment was repeated three times for each drug. The details are listed in the ESI.†

2.3.2 Antifungal activity *in vivo*. The antifungal effect of compound **Y3** on Ss *in vivo* was studied in an artificial climate box (temperature: 20 °C, relative humidity: 80%, light: 14 h, dark: 10 h) through leaf separation experiment.[33]

2.3.3 Anti-TMV activity *in vivo*. The antiviral effect of the target compounds **Y1–Y28** *in vivo* was evaluated by the method reported in the literature.[34,35] The lead compound myricetin and commercial antiviral agent ningnanmycin were used as positive control, and the experiment was repeated three times for each drug. The details are listed in the ESI.†

2.4 Determination of release of cellular contents

Release of cellular contents test of **Y3** against Ss was carried out by the method reported in the literature.[33,36]

2.5 Determination of cell membrane permeability

The determination experiment of **Y3** on the cell membrane permeability of Ss was carried out by the method reported in the literature.[33,36]
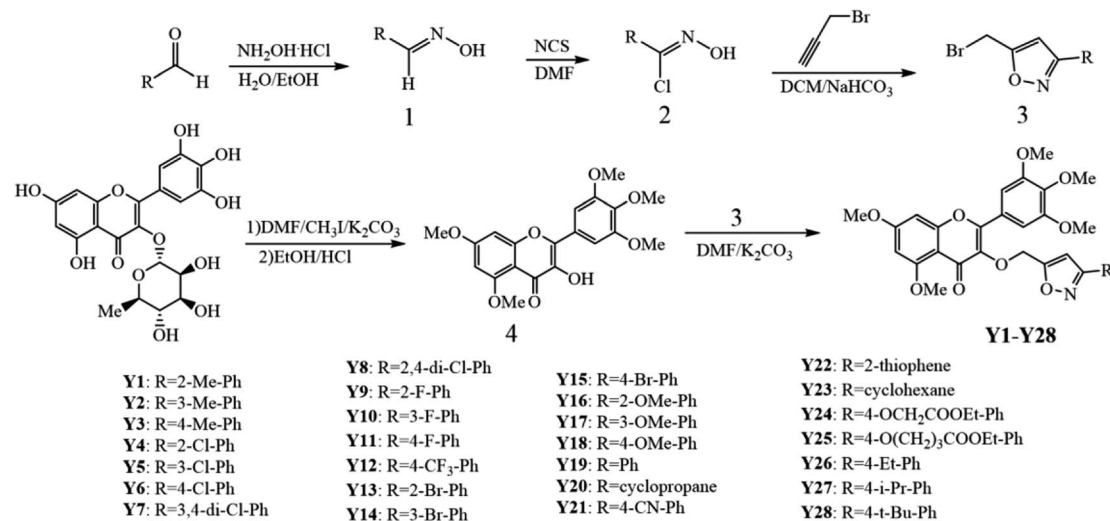
2.6 Microscale thermophoresis

According to the methods reported in the literature,[37] the binding affinity of **Y18**, myricetin and ningnanmycin to TMV-CP was determined by MST.

2.7 Molecular docking

The crystal structure of TMV-CP (PDB ID: 1EI7) was obtained from the protein database (PDB, https://www.rcsb.org).[38] Discovery Studio software was used to simulate molecular docking, and minimization (QM-MM) module was used to optimize the molecular structure.[39] Pymol software was used for visual analysis of molecular docking.

Scheme 1 Synthetic route of the target compounds Y1–Y28.

Table 1 EC$_{50}$ value of target compound against 3 fungi[a]

Pathogen	Chemical	Toxic regression equation	r	EC$_{50}$ (μg mL^{-1})
Bc	**Y3**	$y = 1.1029x + 3.2374$	0.9025	39.6 ± 1.8
	Krm[b]	$y = 0.9655x + 3.6361$	0.9874	25.9 ± 2.2
Pc[1]	**Y3**	$y = 1.3297x + 2.7953$	0.9759	45.5 ± 2.2
	Krm	$y = 0.6592x + 4.3895$	0.9867	8.4 ± 1.9
	Azo[b]	$y = 1.0909x + 3.5486$	0.9729	21.4 ± 2.0
Ss	**Y3**	$y = 0.9234x + 3.9640$	0.9867	13.2 ± 2.1
	Krm	$y = 1.0383x + 3.2701$	0.9907	46.4 ± 2.1
	Azo	$y = 0.8806x + 3.8002$	0.9849	23.0 ± 2.8

[a] Repeat the experiment three times. [b] Commercial antifungal agent kresoxim-methyl (Krm) and azoxystrobin (Azo) were used as positive control.

3. Results and discussion

3.1 Chemistry

The synthesis procedure of the target compounds **Y1–Y28** is shown in Scheme 1, and their spectral data were characterized by NMR and HRMS. And the spectral data of the target compounds can be obtained from the ESI.†

3.2 Purity and state analysis of compound Y1

The purity of **Y1** was analyzed by HPLC, as shown in Fig. S1.† The microstructure of **Y1** was observed at 1500 times by optical microscope, **Y1** was needle-like, and the appearance state of **Y1** was observed indoors, as a white solid, as shown in Fig. S2.† These materials can be offered by ESI.†

3.3 Bioactivity and mechanism of action studies

3.3.1 Antifungal activity *in vitro*. As shown in Table S1†, the inhibitory effect of target compounds **Y1–Y28** on 12 fungi were evaluated by *in vitro* antifungals, and some target compounds showed good antifungal activity. The inhibition rate of **Y3** on Bc was 75.8% *in vitro*, which was better than that of the commercial antifungal agent kresoxim-methyl (69.3%). The inhibition rate

of **Y3** on Pc was 67.7% *in vitro*, which was better than that of kresoxim-methyl (61.1%) and azoxystrobin (63.6%). The inhibition rate of **Y3** on Ss was 81.1% *in vitro*, which was better than that of kresoxim-methyl (62.8%) and azoxystrobin (70.3%). At this concentration, **Y3** showed broad-spectrum antifungal activity.

According to the preliminary biological activity test, the EC$_{50}$ values of **Y3** against three fungi were further tested (Table 1). **Y3** had obvious inhibitory effect on Ss, EC$_{50}$ value was 13.24 μg mL^{-1} exceeding kresoxim-methyl (46.35 μg mL^{-1}) and azoxystrobin (23.04 μg mL^{-1}). **Y3** showed concentration dependence on Pc and Bc.

Table 2 Protective activity of **Y3** against Ss in *ex vivo* leaves of rapeseed[a]

Chemicals	Treatment (μg mL^{-1})	Lesion length (cm)	Control efficacy (%)
Y3	200	1.30 ± 0.13	69.2
Azo[b]	200	0.93 ± 0.08	83.3
Blank control	—	3.10 ± 0.29	—

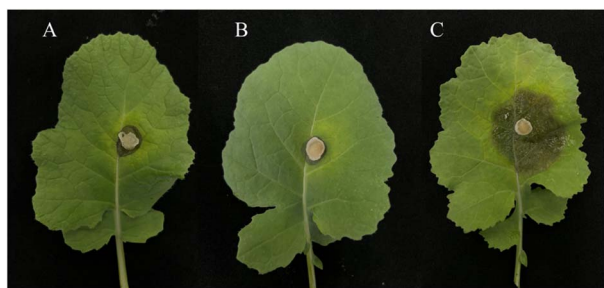[a] Average value of three experiments. [b] The control azoxystrobin.

Fig. 2 Anti-Ss protection efficacy of **Y3** in *ex vivo* leaves of rapeseed. (A) Sprayed with **Y3**; (B) sprayed with azoxystrobin; (C) blank control.

3.3.2　Antifungal activity *in vivo*. *In vitro* antifungal showed that **Y3** had a good inhibitory effect on Ss, and the antifungal activity of **Y3** against Ss *in vivo* was further evaluated. The experimental results are shown in Table 2and Fig. 2, **Y3** had good protective activity *in vivo* against *ex vivo* leaves on the 4th day after inoculation, and the control effect on *ex vivo* leaves was 69.2% at 200 μg mL^{-1}, which was lower than that of the commercialized fungicide azoxystrobin (83.3%).

3.3.3　Effects of Y3 on release of cellular contents. The changes of nucleic acid and protein concentrations in suspension of Ss mycelia were evaluated by measuring the absorbance at 260 and 280 nm. As shown in Fig. 3A and B, compared with the control group, the experimental group treated with **Y3** had a significant increase in nucleic acid and protein release, and was positively correlated with the concentration of **Y3**.
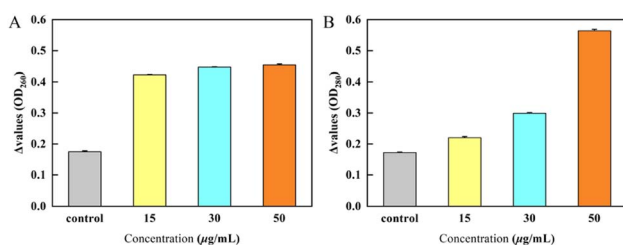

Fig. 3 Release of cellular contents from Ss after treatment with **Y3**. ((A) leakages of nucleic acids; (B) soluble proteins).
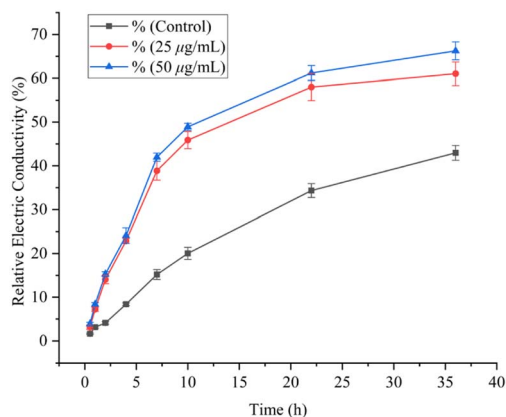
Table 3 Anti-TMV activity of target compounds *in vivo*[a]

Compd	R	Curation	Protection	Inactivation
Y1	2-Me-Ph	52.8 ± 3.2	40.9 ± 6.3	44.5 ± 1.4
Y2	3-Me-Ph	46.2 ± 6.1	49.3 ± 3.3	46.7 ± 2.5
Y3	4-Me-Ph	44.0 ± 6.9	43.8 ± 0.8	56.6 ± 7.6
Y4	2-Cl-Ph	55.7 ± 3.1	52.2 ± 3.5	54.0 ± 3.0
Y5	3-Cl-Ph	30.8 ± 6.5	46.0 ± 5.8	50.7 ± 5.6
Y6	4-Cl-Ph	53.5 ± 1.6	55.8 ± 1.6	53.5 ± 1.4
Y7	3,4-Di-Cl-Ph	47.1 ± 5.0	59.7 ± 6.6	41.9 ± 2.7
Y8	2,4-Di-Cl-Ph	36.9 ± 0.6	56.5 ± 7.7	58.2 ± 5.6
Y9	2-F-Ph	50.0 ± 6.1	50.3 ± 8.7	53.0 ± 3.2
Y10	3-F-Ph	40.3 ± 6.8	52.5 ± 6.6	34.8 ± 6.2
Y11	4-F-Ph	48.4 ± 1.7	39.8 ± 2.6	48.9 ± 5.3
Y12	4-CF$_3$-Ph	38.5 ± 5.5	46.3 ± 3.6	53.3 ± 4.1
Y13	2-Br-Ph	33.8 ± 3.5	59.8 ± 5.4	42.2 ± 3.2
Y14	3-Br-Ph	56.2 ± 1.6	65.0 ± 0.8	56.2 ± 5.5
Y15	4-Br-Ph	34.3 ± 8.2	64.1 ± 3.8	41.8 ± 3.4
Y16	2-OMe-Ph	48.6 ± 3.2	62.8 ± 2.4	62.6 ± 4.0
Y17	3-OMe-Ph	36.0 ± 6.9	43.2 ± 6.0	56.0 ± 6.8
Y18	4-OMe-Ph	60.6 ± 1.6	67.5 ± 5.5	60.4 ± 4.6
Y19	Ph	33.5 ± 7.8	55.8 ± 8.2	57.2 ± 3.8
Y20	Cyclopropane	49.5 ± 3.4	62.2 ± 5.7	53.4 ± 2.8
Y21	4-CN-Ph	53.6 ± 2.6	48.0 ± 0.3	52.6 ± 5.4
Y22	2-Thiophene	48.6 ± 7.8	41.2 ± 2.4	47.9 ± 5.3
Y23	Cyclohexane	32.5 ± 5.5	42.5 ± 3.8	38.1 ± 8.3
Y24	4-OCH$_2$COOEt-Ph	29.1 ± 3.1	46.9 ± 2.5	45.0 ± 1.3
Y25	4-O(CH$_2$)$_3$COOEt-Ph	41.5 ± 3.8	55.7 ± 4.8	39.7 ± 3.0
Y26	4-Et-Ph	53.2 ± 4.4	54.0 ± 4.9	49.9 ± 4.3
Y27	4-i-Pr-Ph	49.1 ± 7.3	31.9 ± 2.5	55.8 ± 3.2
Y28	4-*t*-Bu-Ph	40.8 ± 6.5	44.1 ± 2.3	43.7 ± 4.8
Myricetin		41.4 ± 3.2	43.6 ± 4.1	44.9 ± 3.6
NNM[b]		55.7 ± 1.0	65.3 ± 2.7	92.4 ± 1.8

[a] Average value of three experiments. [b] The control ningnanmycin.

3.3.4　Effect of Y3 on cell membrane permeability. Cell membranes are important for maintaining the integrity of cell structures and normal life activities. The permeability of cell
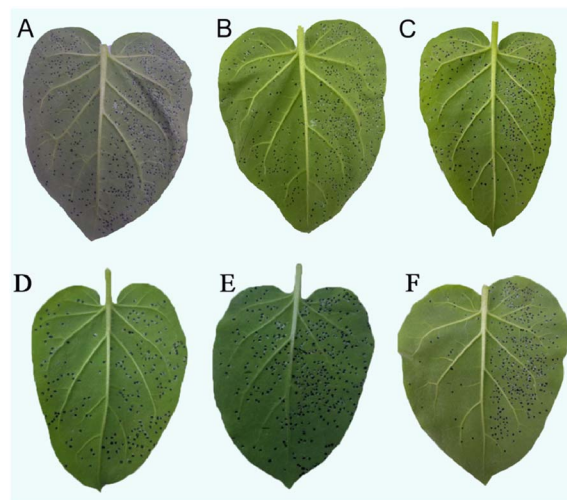

Fig. 4 Determination of cell membrane permeability of **Y3** anti-Ss.

Fig. 5 Morphological effects of **Y18** and ningnanmycin on TMV. **Y18** ((A) Curation, (B) protection, (C) inactivation); ningnanmycin ((D) curation, (E) protection, (F) inactivation)) (left lobe: drug treated; right lobe: blank control).

Table 4 EC$_{50}$ of anti-TMV with some target compounds

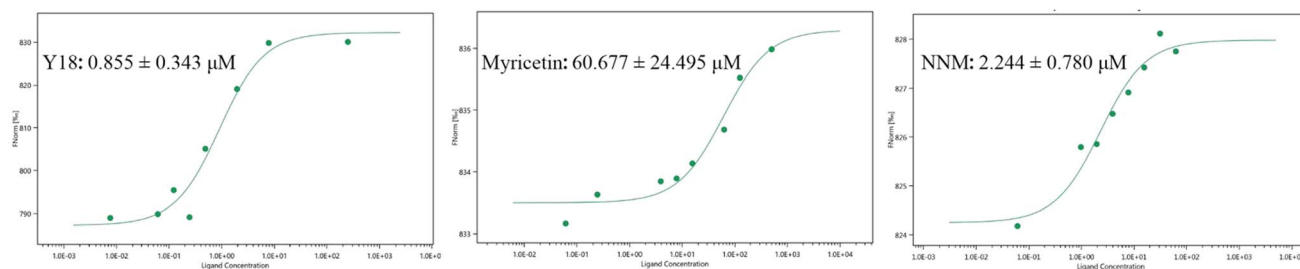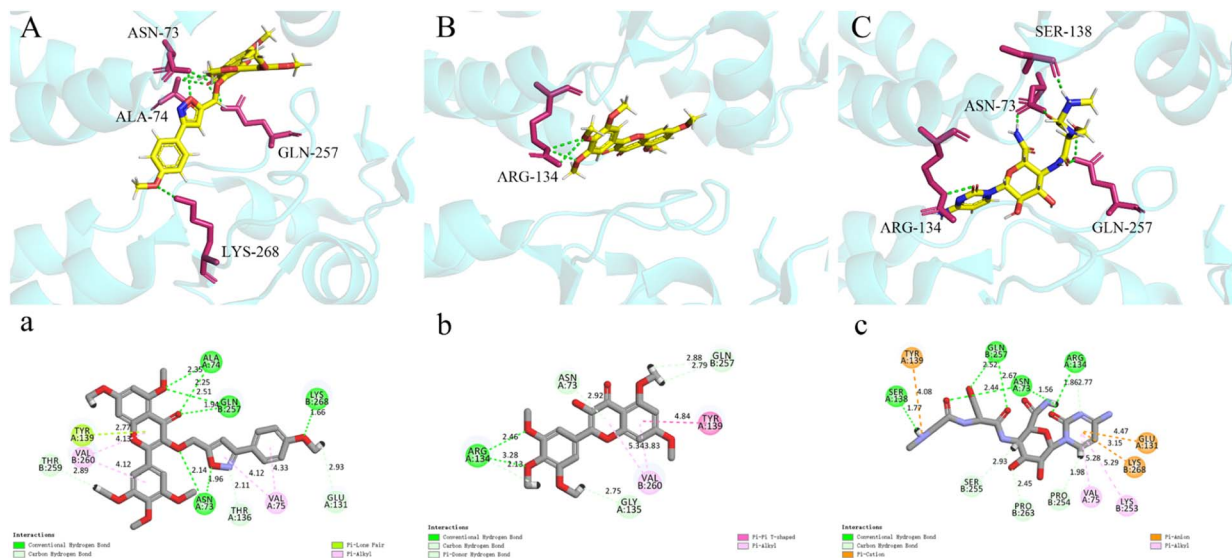| Activity	Compd	Regression equation	r	EC$_{50}$ (μg mL^{-1})
Curative activity	**Y14**	$y = 1.0549x + 2.3572$	0.9952	320.1 $\pm$ 2.1
	Y18	$y = 1.1377x + 2.2042$	0.9986	286.7 $\pm$ 3.0
	NNM	$y = 0.9046x + 2.7228$	0.9898	329.1 $\pm$ 3.2
Protective activity	**Y18**	$y = 1.4022x + 1.7434$	0.9909	210.1 $\pm$ 4.5
	NNM	$y = 1.2083x + 2.1456$	0.9834	230.3 $\pm$ 3.7

membrane can be evaluated by relative conductivity. As shown in Fig. 4, the relative conductivity of mycelium in the experimental group treated with **Y3** increased significantly over 7 h. Over time, the relative conductivity was much higher than in the control group. In addition, the increase in drug concentration makes the increase in conductivity more pronounced. This result shows that **Y3** can cause the destruction of the hyphal cell membrane, which in turn leads to the death of the hyphae.

3.3.5 Anti-TMV activity *in vivo*. The anti-TMV activity of the target compounds **Y1–Y28** was evaluated by antiviral *in vivo* as shown in Table 3. The curative, protective and inactivating activities of **Y1–Y28** were 29.1–60.6%, 31.9–67.7% and 34.8–62.6%, respectively. Among them, **Y18** had the best curative and

protective activity, 60.6 and 67.5%, respectively, which was superior to ningnanmycin (57.7 and 65.3%). The *in vitro* effects of **Y18** and ningnanmycin on TMV are shown in Fig. 5.

In addition, the EC$_{50}$ values of **Y14** and **Y18** with good antiviral activity were further evaluated, as shown in Table 4. The EC$_{50}$ values for the curative activity of **Y14** and **Y18** anti-TMV were 320.1 and 286.7 μg mL^{-1}, respectively, superior to ningnanmycin (329.1 μg mL^{-1}). The EC$_{50}$ value of **Y18** anti-TMV protective activity was 210.1 μg mL^{-1}, which was better than ningnanmycin (230.3 μg mL^{-1}).

3.3.6 Microscale thermophoresis. Fig. 6 shows the MST results of **Y18**, myricetin, ningnanmycin and TMV-CP. The binding affinity can be evaluated by K_d value. The K_d values of

Fig. 6 The MST results of **Y18**, myricetin and ningnanmycin to TMV-CP.

Fig. 7 Molecular docking of **Y18**, myricetin, and ningnanmycin to TMV-CP. **Y18** (A, a), myricetin (B, b), ningnanmycin (C, c).

the three combined with TMV-CP were 0.855 ± 0.343, 60.677 ± 24.495 and 2.244 ± 0.780 μM, respectively. **Y18** showed strong binding ability with TMV-CP, which was much stronger than the lead compound myricetin and the control drug ningnanmycin.

The results showed that the binding affinity of myricetin to TMV-CP was significantly enhanced after heterocyclic modification with isoxazole.

3.3.7 Molecular docking. Molecular docking was used to identify the identification sites of **Y18**, myricetin and ningnanmycin with TMV-CP. The results are shown in Fig. 7, and the three were well embedded in the active pocket of TMV-CP. **Y18** had 7 conventional hydrogen bonds with TMV-CP, in which the oxygen atom on the isoxazole fragment and the oxygen atom on the methoxy group interact firmly with the amino acid residues ASN73 and LYS268 through two conventional hydrogen bonds (1.96 Å, 1.66 Å), respectively. There were 3 conventional hydrogen bonds and 6 conventional hydrogen bonds in myricetin and ningnanmycin and TMV-CP, respectively, and the number of hydrogen bonds was lower than that of **Y18**. In addition, **Y18** binds well to amino acid residues ALA74, TYR139, GLU131 and VAL75 by conventional hydrogen bonding, pi-lone pair, carbon–hydrogen bonding, and pi-alkyl, respectively. Previous studies have reported that such amino acid residues play a key role in the self-assembly of TMV particles,[40,41] and **Y18** may hinder the self-assembly of TMV particles. The molecular docking results were consistent with the bioassay activity. Based on the molecular docking results of **Y18**, myricetin and ningnanmycin well verified the good antiviral activity of **Y18**.

4. Conclusion

A series of myricetin derivatives containing isoxazole were designed and synthesized, and the activity of all synthetic compounds against 12 plant-derived fungi and anti-TMV was evaluated. The antifungal activity showed that the EC_{50} value of **Y3** for Ss was 13.24 μg mL^{-1} was superior to azoxystrobin and kresoxim-methyl. Release of cellular contents and cell membrane permeability experiments further revealed that **Y3** causes destruction of the cell membrane of hyphae. The results of *in vivo* antiviral activity test showed that **Y18** had the best curative and protective activity, and the EC_{50} values were 286.6 and 210.1 μg mL^{-1}, respectively, which were better than ningnanmycin (329.1 and 230.3 μg mL^{-1}). The MST results showed that **Y18** had a strong binding affinity with TMV-CP. The molecular docking results further revealed that **Y18** may hinder the self-assembly of TMV particles. In summary, myricetin derivatives containing isoxazole backbones can serve as potential antifungal, antiviral drug molecules.

Conflicts of interest

The authors declare no competing financial interest.

Acknowledgements

References

1 M. V. Nguyen, J. W. Han, H. Kim and G. J. Choi, *ACS Omega*, 2022, **7**, 33273–33279.

2 Z. W. Wang, Q. Peng, X. Gao, S. Zhong, Y. Fang, X. L. Yang, Y. Ling and X. Liu, *J. Agric. Food Chem.*, 2020, **68**, 5318–5326.

3 R. N. Silva, V. N. Monteiro, A. S. Steindorff, E. V. Gomes, E. F. Noronha and C. J. Ulhoa, *Fungal Biol.*, 2019, **123**, 565–583.

4 P. Y. Wang, M. W. Wang, D. Zeng, M. Xiang, J. R. Rao, Q. Q. Liu, L. W. Liu, Z. B. Wu, Z. Li, B. A. Song and S. Yang, *J. Agric. Food Chem.*, 2019, **67**, 3535–3545.

5 X. Zhou, Y. Q. Ye, S. S. Liu, W. B. Shao, L. W. Liu, S. Yang and Z. B. Wu, *Pestic. Biochem. Physiol.*, 2021, **172**, 104749.

6 C. Buttimer, O. McAuliffe, R. P. Ross, C. Hill, J. O'Mahony and A. Coffey, *Front. Microbiol.*, 2017, **8**, 34.

7 S. K. Wu, J. Shi, J. X. Chen, D. Y. Hu, L. S Zang and B. A. Song, *J. Agric. Food Chem.*, 2021, **69**, 4645–4654.

8 X. Tang, C. Zhang, M. Chen, Y. N. Xue, T. T. Liu and W. Xue, *New J. Chem.*, 2020, **44**, 2374–2379.

9 T. T. Liu, F. Peng, X. Cao, F. Liu, Q. F. Wang, L. W. Liu and W. Xue, *ACS Omega*, 2021, **6**, 30826–30833.

10 Z. Javed, K. Khan, J. Herrera-Bravo, S. Naeem, M. J. Iqbal, Q. Raza, H. Sadia, S. Raza, M. Bhinder, D. Calina, J. Sharifi-Rad and W. C. Cho, *Cancer Cell Int.*, 2022, **22**, 239.

11 S. C. Iyer, A. Gopal and D. Halagowder, *Mol. Cell. Biochem.*, 2015, **407**, 223–237.

12 S. Pasetto, V. Pardi and R. M. Murata, *PLoS One*, 2014, **9**, e115323.

13 M. S. Yu, J. Lee, J. M. Lee, Y. Kim, Y. W. Chin, J. G. Jee, Y. S. Keum and Y. J. Jeong, *Bioorg. Med. Chem. Lett.*, 2012, **22**, 4049–4054.

14 X. W. Su and D. H. D'Souza, *Food Environ. Virol.*, 2013, **5**, 97–102.

15 R. Bertin, Z. Chen, R. Marin, M. Donati, A. Feltrinelli, M. Montopoli, S. Zambon, E. Manzato and G. Froldi, *Biomed. Pharmacother.*, 2016, **82**, 472–478.

16 Y. Tong, X. M. Zhou, S. J. Wang, Y. Yang and Y. L. Cao, *Arch. Pharmacal Res.*, 2009, **32**, 527–533.

17 K. C. Medeiros, C. A. Figueiredo, T. B. Figueredo, K. R. Freire, F. A. Santos, N. M. Alcantara-Neves, T. M. Silva and M. R. Piuvezam, *J. Ethnopharmacol.*, 2008, **119**, 41–46.

18 S. C. Jiang, S. J. Su, M. Chen, F. Peng, Q. Zhou, T. T. Liu, L. W. Liu and W. Xue, *J. Agric. Food Chem.*, 2020, **68**, 5641–5647.

19 V. Basavanna, S. Doddamani, M. Chandramouli, U. K. Bhadraiah and S. Ningaiah, *J. Iran. Chem. Soc.*, 2022, **19**, 3249–3283.

20 G. C. Arya, K. Kaur and V. Jaitak, *Eur. J. Med. Chem.*, 2021, **221**, 113511.

21 M. B. Bommagani, J. R. Yerrabelly, M. Chitneni, G. Thalari, N. R. Vadiyala, S. K. Boda and P. R. Chitneni, *Chem. Data Collect.*, 2021, **31**, 100629.

© 2023 The Author(s). Published by the Royal Society of Chemistry

22 A. Egorova, E. Kazakova, B. Jahn, S. Ekins, V. Makarov and M. Schmidtke, *Eur. J. Med. Chem.*, 2020, **188**, 112007.

23 P. Kumar Kushwaha, K. Saurabh Srivastava, N. Kumari, R. Kumar, D. Mitra and A. Sharon, *Bioorg. Med. Chem.*, 2022, **56**, 116612.

24 G. Saravanan, V. Alagarsamy and P. Dineshkumar, *Arch. Pharmacal Res.*, 2021, **44**, 1–11.

25 F. Liu, M. Y. Wang, X. H. Teng, P. Z. Zhang and L. Jiang, *Res. Chem. Intermed.*, 2013, **40**, 1575–1581.

26 R. F. Sun, Y. Q. Li, L. S. Xiong, Y. X. Liu and Q. M. Wang, *J. Agric. Food Chem.*, 2011, **59**, 4851–4859.

27 X. L. Sun, Z. M. Ji, S. P. Wei and Z. Q. Ji, *J. Agric. Food Chem.*, 2020, **68**, 15107–15114.

28 L. Schwarz, U. Girreser and B. Clement, *Eur. J. Org. Chem.*, 2014, **2014**, 1961–1975.

29 H. Huang, P. Si, L. Wang, Y. Xu, X. Xu, J. Zhu, H. L. Jiang, W. H. Li, L. L. Chen and J. Li, *ChemMedChem*, 2015, **10**, 1184–1199.

30 A. V. Serebryannikova, E. E. Galenko, M. S. Novikov and A. F. Khlebnikov, *Tetrahedron*, 2021, **88**, 132153.

31 W. Xue, B. A. Song, H. J. Zhao, X. B. Qi, Y. J. Huang and X. H. Liu, *Eur. J. Med. Chem.*, 2015, **97**, 155–163.

32 X. M. Tang, Q. Zhou, W. L. Zhan, D. Hu, R. Zhou, N. Sun, S. Chen, W. N. Wu and W. Xue, *RSC Adv.*, 2022, **12**, 2399–2407.

33 X. D. Yin, K. Y. Ma, Y. L. Wang, Y. Sun, X. F. Shang, Z. M. Zhao, R. X. Wang, Y. J. Chen, J. K. Zhu and Y. Q. Liu, *J. Agric. Food Chem.*, 2020, **68**, 11096–11104.

34 T. T. Liu, F. Peng, Y. Y. Zhu, X. Cao, Q. F. Wang, F. Liu, L. W. Liu and W. Xue, *Arabian J. Chem.*, 2022, **15**, 104019.

35 X. H. Gan, D. Y. Hu, Y. J Wang, L. Yu and B. A. Song, *J. Agric. Food Chem.*, 2017, **65**, 4367–4377.

36 D. Y. Ma, D. C. Ji, Z. Q. Zhang, B. Q. Li, G. Z. Qin, Y. Xu, T. Chen and S. P. Tian, *Postharvest Biol. Technol.*, 2019, **150**, 158–165.

37 T. Guo, R. J Xia, M. Chen, J. He, S. J. Su, L. W. Liu, X. Y. Li and W. Xue, *RSC Adv.*, 2019, **9**, 24942–24950.

38 Y. Chen, P. Li, S. J. Su, M. Chen, J. He, L. W. Liu, M. He, H. Wang and W. Xue, *RSC Adv.*, 2019, **9**, 23045–23052.

39 D. X. Luo, S. X. Guo, F. He, S. H. Chen, A. L. Dai, R. F. Zhang and J. Wu, *J. Agric. Food Chem.*, 2020, **68**, 7226–7234.

40 A. C. Bloomer, J. N. Champness, G. Bricogne, R. Staden and A. Klug, *Nature*, 1978, **276**, 362–368.

41 Y. Y. Wang, F. Z. Xu, Y. Y. Zhu, B. A. Song, D. X. Luo, G. Yu, S. H. Chen, W. Xue and J. Wu, *Bioorg. Med. Chem. Lett.*, 2018, **28**, 2979–2984.